Effects of Arctic freshwater forcing on thermohaline circulation during the Pleistocene

Jochen Knies Geological Survey of Norway, Leiv Eirikssons vei 39, NO-7491 Trondheim, Norway
Jens Matthiessen, Andreas Mackensen, Ruediger Stein — Alfred Wegener Institute for Polar and Marine Research (AWI), Columbusstrasse, D-27568 Bremerhaven, Germany
Christoph Vogt, Thomas Frederichs — University of Bremen, Klagenfurter Strasse, D-28359 Bremen, Germany
Seung-Il Nam Korea Institute of Geoscience and Mineral Resources, 305-350 Daejeon, Korea

ABSTRACT

In this paper, we make use of calcium carbonate-bearing sediment sequences in the Arctic-Atlantic gateway to produce a standard reference climate record for the Arctic Ocean. We present a continuous and exceptionally well-dated marine sediment record documenting the strong imprint of Arctic freshwater pulses on Earth's climate system throughout the past 0.8 m.y. Planktic foraminiferal oxygen and carbon isotope data reveal that freshwater plumes released from collapsing circum-Arctic ice sheets and ice-dammed lakes were advected to the Arctic Ocean gateway on sub-Milankovitch time scales. Given the close correspondence of Arctic freshwater pulses and strength of North Atlantic Deep Water formation as inferred from carbon isotope data, we conclude that freshening of the Arctic Ocean influenced thermohaline circulation more frequently than previously recognized. Our data show that it is critical for coupled atmosphere-ice-ocean general circulation models aimed at unraveling climate forcing factors during the Pleistocene to consider Arctic freshwater as a crucial forcing factor.

Keywords: Arctic Ocean, Pleistocene, isotopes, freshwater.

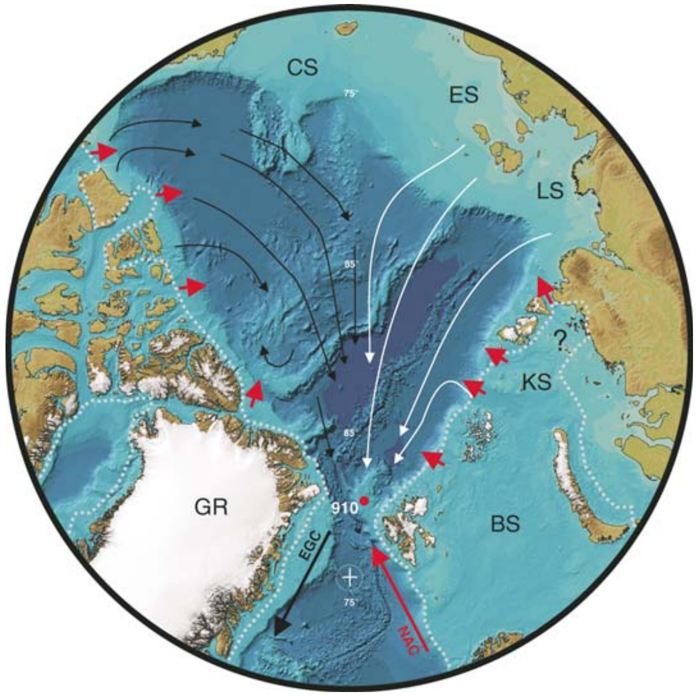

Figure 1. Bathymetry of the Arctic–North Atlantic sector, the location of Ocean Drilling Program (ODP) Site 910 (80°15.882°N, 6°35.405°E; 556.4 m water depth), and the approximate position of the LGM ice sheet (dotted lines) (Dyke et al., 2002; Svendsen et al., 2004). Black arrows—postulated Arctic ice-drift pattern during glacial intervals (Bischof and Darby, 1997); white arrows—modern ice-drift pattern in the Eurasian Arctic sector; red arrows—major freshwater drainage outlets during the last glacial cycle. Crosses indicate zones of modern deep/intermediate water formation in the Greenland Sea. EGC—East Greenland Current; NAC—North Atlantic Current; GR—Greenland; BS—Barents Sea; KS—Kara Sea; LS—Laptev Sea; ES—East Siberian Sea; CS—Chukchi Sea.

INTRODUCTION

Modern observations of Arctic Ocean freshening attributed to enhanced Eurasian river discharge in response to global warming (Peterson et al., 2006) have potentially large implications for changes in the Atlantic meridional overturning circulation (AMOC). Numerical model simulations have confirmed the sensitivity of the circulation to freshwater input from (sub)polar sources (Ganopolski and Rahmstorf, 2001). Freshwater-induced weakening of thermohaline circulation is often inferred to have caused abrupt climate changes during the last glacial cycle. Direct forcing from the Arctic Ocean is therefore a critical but largely unknown component.

Results from borehole and modeling studies during extreme Cenozoic "snapshots" of climate change highlight the enormous impact of Arctic freshwater forcing on Earth's climate development (Brinkhuis et al., 2006). For the latest Pleistocene (<0.18 Ma), climate proxy data have demonstrated the Arctic Ocean's role in freshening the gateway region during periods of major ice-sheet collapse (Spielhagen et al., 2004). Timing and duration of Arctic freshwater perturbations beyond the last 0.18 m.y., however, are currently more speculative, and records assessing the potential impact of freshwater on (sub)Milankovitch time scales in the Pleistocene Arctic Ocean are not yet available. A primary reference section for pinpointing the climate-induced modulations of the hydrological regime in the eastern sector of the Eurasian Basin for the last 0.8 m.y. has been recovered by Ocean Drilling Program (ODP) Leg 151 Hole 910A from the marginal eastern Arctic Ocean (Yermak Plateau) (Fig. 1; Myhre et al., 1995). In particular, this section will allow us to constrain the occurrence and magnitude of Arctic freshwater forcing during the Pleistocene. Previous studies (Hole 910A) confirm that carbonate-bearing sequences in the vicinity of the Atlantic–Arctic Ocean gateway permit the establishment of a relatively continuous stable oxygen isotope stratigraphy within the Brunhes Chron.

We present a continuous stack of new and supplemented (Flower, 1997) stable oxygen and carbon isotope data of the planktic (surface dwelling) foraminifera *Neogloboquadrina pachyderma*, sinistral coiling (*N. pachyderma* sin.) in Hole 910A; these data allow us to evaluate Arctic freshwater influence. *N. pachyderma* sin. $\delta^{18}O$ values mainly reflect regional salinity variations in the upper water column of the Arctic Ocean, giving a calcification depth between 100 and 200 m, depending on the depth of the pycnocline (Bauch et al., 1997), that causes small amplitudes in the $\delta^{18}O$ record during glacial/interglacial cycles (Nørgaard-Pedersen et al., 2003). Downcore deviations from the global pattern have regularly been used to identify $\delta^{18}O$-depleted meltwater events during glacial terminations and/or collapses of ice-dammed lakes in the circum-Arctic throughout the past 0.18 m.y. (Spielhagen et al., 2004). Accompanying low $\delta^{13}C$ values support changes in water mass properties of surface waters in the Arctic Ocean, and are indicative of an inhibited vertical water mass exchange due to stratification from a surficial low-salinity freshwater lid. Freshwater pulses thus contribute to a lowering of the $\delta^{13}C$ values in *N. pachyderma* sin., after the particular depth habitat becomes affected. Accordingly, coupled excursions to light $\delta^{18}O$ and light $\delta^{13}C$ values of *N. pachyderma* (sin.) in Hole 910A yield strong evidence of Arctic freshwater pulses to the gateway region.

METHODOLOGY

Hole 910A was drilled in 556.4 m water depth on the southern Yermak Plateau (80°15.882°N, 6°35.405°E). In total, 34 m of almost undisturbed Pleistocene sediments were cored, and recovery was, on the average, 71%, but 98% from 0 to 24.5 m below seafloor (mbsf) (Myhre et al., 1995). The new stable isotope data set of *N. pachyderma* (sin.) tests (125–250 µm) was generated at the Alfred Wegener Institute using a Finnigan MAT 251 isotope ratio gas mass spectrometer, directly coupled to an automated carbonate preparation device (Kiel II) and calibrated using NIST19 international standard to the Vienna Peedee belemnite (VPDB). The precision of the measurements at 1σ based on repeated analyses of an internal laboratory standard (Solnhofen limestone) was better than ±0.08‰ and ±0.06‰ for oxygen and carbon isotopes, respectively. For constructing a stable isotope stratigraphy of Hole 910A, the data published by Flower (1997) and analyzed at the University of California–Santa Cruz, were combined with the newly generated and extended data presented here. Because the previously published data were reported versus NBS19 values of −1.85‰ for $\delta^{18}O$ and 2.03‰ for $\delta^{13}C$, we adjusted the oxygen isotope values to the VPDB scale (–2.20‰) by adding 0.35‰. No further corrections or adjustments were applied. The temporal resolution of the stable isotope record, including previously sampled intervals (Flower, 1997), is now 2,000–3,000 yr. All data are stored in the World Data Center for Marine Environmental Sciences (http://www.wdc-mare.org).

Discrete oriented samples for paleomagnetic measurements were taken in cubic boxes (6.2 cm^3) from the archive at 5 cm intervals from Core 1H1–3HCC (0–19.5 mbsf), whereas the archive halves of Core 4H1–4HCC (19.5–24.5 mbsf) were measured continuously. The discrete samples were analyzed at the Department of Geosciences, University of Bremen. Paleomagnetic directions and magnetization intensities were measured on a cryogenic magnetometer (model 2G Enterprises 755 HR). Natural remanent magnetization (NRM) was measured on each sample before these were subjected to a systematic demagnetization treatment involving 16 steps for each sample, with a maximum alternating field intensity of 100 mT. A detailed vector analysis was applied to the results to determine the characteristic remanent magnetization (ChRM). The continuous measurements on the archive halves were conducted at the Leibniz Institute for Applied Geosciences in Grubenhagen. The samples were stepwise demagnetized in an alternating field (AF) in a superconducting rock magnetometer (SRM) system 760–5.0 LC (2G Enterprises). Six steps with a maximum field intensity of 30 mT were applied.

THE AGE MODEL

The chronostratigraphy of Hole 910A was improved relative to Flower (1997) by a multi-proxy chronological approach applying both absolute and relative dating methods (Table DR1 in the GSA Data Repository[1]). Planktic foraminifera and calcareous nannofossil stratigraphy indicate that Site 910 sediments were deposited in the Pleistocene (Myhre et al., 1995). The uppermost sediment sequence is intercalated within an interval with positive inclinations from 0 to ~19.4 mbsf, suggesting that these are excursions within the Brunhes Chron (Fig. 2). Further diagnostic biostratigraphic events for the upper Pleistocene include the highest occurrence of the calcareous nannofossil *Pseudoemiliania lacunosa* in late marine oxygen isotope stage (MIS) 12 (~0.44 Ma) at 10.45 mbsf, and the maximum occurrence of the benthic foraminifera *Pullenia bulloides* in MIS substage 5.1 (0.08 Ma) at 1.95 mbsf (Table DR1). Extrapolation of the mean (2.9 cm/ka) sedimentation rate downcore from the *P. lacunosa* event yields an age of older than 0.9 Ma for 21 mbsf. This is consistent with the placement of the Brunhes/Matuyama boundary (0.78 Ma) at 19.45 mbsf (Fig. 2). The identification of several Brunhes geomagnetic field excursions during this interval supports the age model of Hole 910A (Fig. 2). The interval from 19.5 to 23 mbsf is characterized by variable inclinations corresponding to the upper Matuyama Chron (0.78–0.99 Ma) and the Jaramillo Subchron (0.99–1.07 Ma) (Fig. 2). A hiatus (ca. 0.79–0.95 Ma) inferred from the millimeter-scale sedimenta-

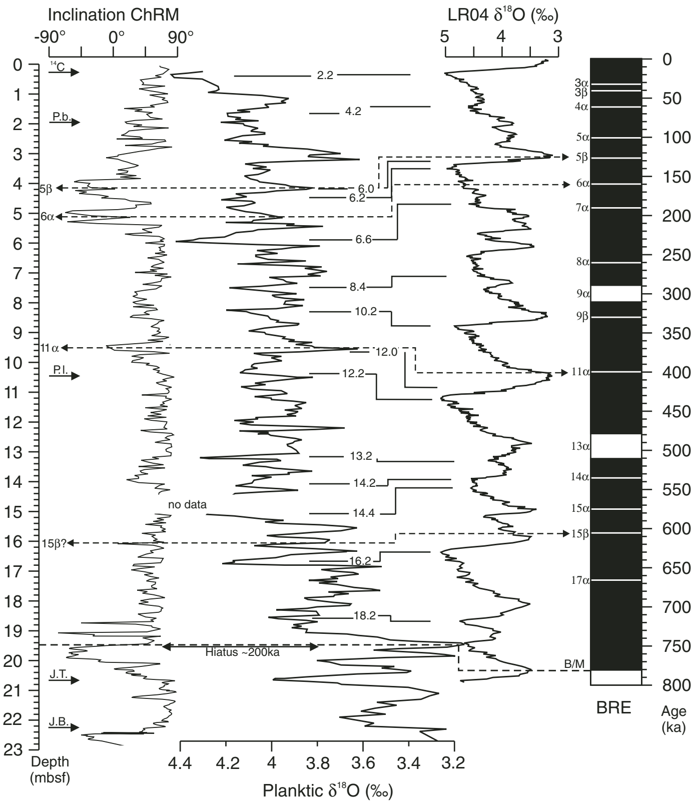

Figure 2. Chronostratigraphy of Hole 910A: Downcore variation of ChRM inclinations and (three-point smoothed) stable oxygen isotope ($\delta^{18}O$) values of *Neogloboquadrina pachyderma* sin. in Hole 910. Right: Late Pleistocene age model of the LR04 stack (Lisiecki and Raymo, 2005) and a global compilation of Brunhes geomagnetic field excursions (Lund et al., 2006). Arrows define first-order age fixpoints, including AMS ^{14}C radiocarbon dates (Sample No. 910A), 1H1A 34–35 cm, 21,800+140/–130 BP (KIA 23036), $\delta^{13}C$-normalized and corrected for reservoir effects equal to 440 yr, biostratigraphic datum (P.b.—*Pullenia bulloides*, P.l.—*Pseudoemiliani lacunosa*), and magnetic (sub)chrons (J.T./J.B—Jaramillo Top/Base) (see Table DR1 [see footnote1]). Brunhes reversal excursions (BRE) are marked by stippled lines (see Lund et al., 2006, for age assignments and references). Oxygen isotope events are marked by arrows and are correlated to LR04 stack. The hiatus (~0.79–0.95 Ma) at the bottom of Hole 910A is marked by arrows. B/M—Brunhes-Matuyama boundary.

[1]GSA Data Repository item 2007268, Table DR1 (age model of ODP Hole 910A) and references, is available online at www.geosociety.org/pubs/ft2007.htm, or on request from editing@geosociety.org or Documents Secretary, GSA, P.O. Box 9140, Boulder, CO 80301, USA.

tion rates at the top of the Matuyama Chron (~19.5 mbsf) is supported by a pronounced change of physical property data in the lower part of Hole 910A (Myhre et al., 1995).

All age-control points down to ~0.8 Ma are used to correlate the stacked δ^{18}O record of Hole 910A to a δ^{18}O reference curve (LR04-stack) (Lisiecki and Raymo, 2005) (Fig. 2). Identification of oxygen-isotope events (Table DR1) is based on the general agreement that heavy δ^{18}O >4‰ associated with relatively heavy δ^{13}C values characterize glacial isotope stages (Fig. 2). Ages are according to Lisiecki and Raymo (2005).

IDENTIFICATION OF ARCTIC OCEAN FRESHWATER PULSES

The stable isotope record of Hole 910A exhibits distinct cycles between heavy and light oxygen isotope values with a gradual decrease to lighter values in the lower part of the hole (Fig. 3). δ^{18}O values range from ~4.4‰ to 3.2‰ from 0 to 19.5 mbsf, with a mean δ^{18}O value of 3.8‰. Arctic freshwater pulses to the gateway region are reflected in the isotopic record as excursions—both low δ^{18}O and δ^{13}C values—of variable amplitude, duration, and regional extent (Fig. 3). Amplitudes in the δ^{18}O record can reach ~0.8‰, but usually are 0.3–0.8‰ and always correspond to low δ^{13}C values (<–0.4‰) (amplitudes <0.3‰ are not considered here).

Well-constrained events during the late Pleistocene include outflow of freshwater from the Barents/Kara ice-dammed lakes at ~0.11, ~0.08–0.075, and 0.052 Ma (Spielhagen et al., 2004). Prominent Arctic freshwater flux to the gateway region is also well known for the last and penultimate deglaciations, when continental ice sheets in the circum-Arctic collapsed and huge

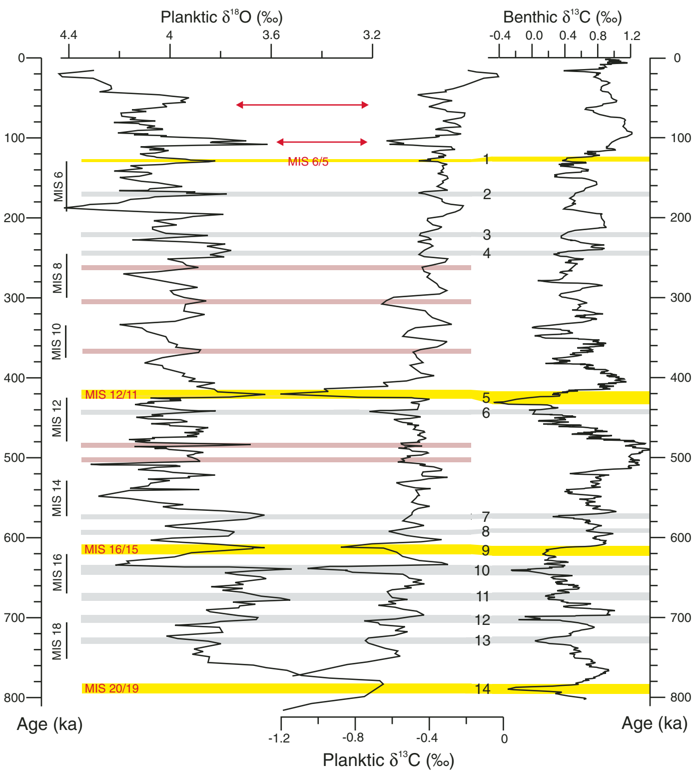

Figure 3. Climate proxy data from the Atlantic-Arctic gateway. Three-point smoothed stable oxygen (δ^{18}O) and carbon (δ^{13}C) isotope values of planktic foraminifera *Neogloboquadrina pachyderma* sin. in Hole 910A versus age. Right: Smoothed benthic δ^{13}C record from the North Atlantic (ODP Site 980, 55°29.1°N, 14°42.1°W) (Flower et al., 2000). Red arrows indicate well-constrained Arctic freshwater pulses during Early Weichselian. Main glacial terminations discussed in the text are marked in yellow. Numbers indicate Arctic freshwater pulses concomitant to the decrease of North Atlantic Deep Water Formation. Pink lines mark regional freshwater pulses in the Arctic Ocean.

amounts of freshwater and icebergs were released into the Arctic Ocean (Darby et al., 2002; Spielhagen et al., 2004). More recently, evidence from proxy data and numerical simulations (Tarasov and Peltier, 2005; Peltier et al., 2006) suggest Arctic freshwater forcing of the Younger Dryas cold reversal. Arctic freshwater discharge during periods of millennial-scale climate instability thus appears to have contributed more frequently to perturbations of AMOC, at least during the last glacial/interglacial cycle. The latter is verified within the youngest portion of Hole 910A, when freshwater injections inferred from excursions in the δ^{18}O and δ^{13}C records (Fig. 3) punctuated the glacial termination during the penultimate deglaciation (MIS 6/5) and the Late Pleistocene (~0.11 Ma, ~0.052 Ma).

ARCTIC OCEAN FRESHWATER PERTURBATION DURING THE LATE PLEISTOCENE

Hence, with the synchronicity of events for regional Arctic freshwater discharge during the last 0.13 m.y., we show that on the order of 14 comparable freshwater events occur throughout the entire Brunhes Chron (Fig. 3). Our coupled δ^{18}O-δ^{13}C records reveal that Arctic freshwater discharge to the gateway region occurred frequently relative to the background of the well-known glacial/interglacial cycle, implying that episodic discharge has contributed to fundamental perturbations of thermohaline circulation during the middle-late Pleistocene. The observed synchronous decrease in North Atlantic Deep Water formation during most Arctic freshwater pulses (Fig. 3) supports this model. Most spectacular are freshwater pulses during glacial terminations (Fig. 3), such as the penultimate deglaciation, MIS 12/11 and MIS 16/15 transitions, as well as on top of the hiatus (MIS 20/19 transition). The disintegration of large ice sheets and the melting of icebergs are inferred to be the main sources for freshwater pulses during these periods. A prominent sequence, including the hiatus (~0.79–0.95 Ma) attributed to a pronounced ice sheet advance (Flower, 1997) or ploughing of deep-draft icebergs (Kristoffersen et al., 2004), and a subsequent distinct freshwater pulse are concurrent with the mid-Pleistocene transition. The latter is characterized by a significant increase in global ice volume from 0.942 to 0.892 Ma relative to the background of low-amplitude obliquity cycles (Mudelsee and Schulz, 1997). The timing of ice collapse and the release of freshwater during the MIS 20/19 transition is presumably consistent with the oldest documented glaciation in northern Eurasia, older than 0.7 Ma (Astakhov, 2004), and can be traced into the Nordic Seas (Helmke et al., 2003), implying a reorganization of ocean circulation triggered primarily by an Arctic freshwater source.

Major freshwater releases during MIS 16/15 and MIS 12/11 transitions are coincident with severe glaciations in the circum-Arctic; both are supported by climate proxy data in the Nordic Seas and Fennoscandia. In particular, the massive ice-sheet expansion during MIS 12 associated with the mid-Brunhes Event, identified both from climate proxy (Helmke et al., 2003) and acoustic data (Rise et al., 2004) in the Nordic Sea region, terminated with a huge freshwater pulse into the Arctic Ocean concomitant with distinct cooling events in the Nordic Seas (Bauch et al., 2000). Moreover, freshwater released by collapsing Arctic ice sheets after the MIS 12 glaciation apparently disturbed the hydrological regime not only in the gateway region but also contributed to destabilization of thermohaline circulation in the North Atlantic during the following termination (Fig. 3). Arctic freshwater and iceberg discharge to the gateway region, and thus freshening of the North Atlantic after major glaciations, appear to have been a dominant pattern over the past 0.8 m.y.

Surprisingly, apart from events associated with major MIS terminations in the circum-Arctic over the past 0.8 m.y., all transitions into glacial and interglacial periods also record freshwater events. This suggests frequent instabilities of ice sheets on Milankovitch and sub-Milankovitch time scales as known from the last glacial cycle (Spielhagen et al., 2004). The prominent δ^{18}O and δ^{13}C excursions independent from glacial or interglacial periods point to additional freshwater plumes that advected through the Arctic gateway directly into the Nordic Seas. The regional significance of these events remains speculative. However, based on the evidence presented in this study, we suggest that waxing and waning of ice sheets in the circum Arctic, and release of freshwater from bursting ice-dammed lakes, are not confined to glacial periods at all. The irregular timing of events is at least consistent with a pattern during the last glacial cycle of gateway freshening owing to ice-sheet collapse and bursting ice-dammed lakes occurring both during glacial terminations and interstadials of MIS 5 (Darby et al., 2002; Spielhagen et al., 2004).

CONCLUSIONS

We show that suborbital-scale variations in Arctic freshwater discharge draining through the gateway into the Nordic Sea were present over the past 0.8 m.y. and indicate a more dynamic coupling between variable Arctic Ocean freshwater flux and perturbations of AMOC than is generally acknowledged. These variations, similar in character and timing to meltwater events during the last glacial cycle, occurred irregularly during glacial terminations, glacial periods, and even interstadial periods, suggesting frequent instabilities of circum-Arctic ice sheets and freshwater discharge on sub-Milankovitch time scales. These findings confirm speculations that the relative influence of Arctic versus North Atlantic source waters on the stability of Nordic Sea water masses has frequently changed during the Pleistocene (Raymo et al., 2004). For instance, by assuming a massive flow of low-saline polar surface water through Fram Strait, the suppression of anticyclonic eddies that occur today in the central Greenland Sea (Gascard et al., 2002) would have prevented an important pathway for ventilation of the deep North Atlantic. This is similar to modern times, when increased Arctic gateway ice export resulted in the "Great Salinity Anomaly" (GSA) (Dickson et al., 1988) and slowed down formation of Greenland Deep Water formation in the late 1970s and early 1980s. Hence, we conclude that Arctic freshwater discharge is critical for coupled atmosphere-ice-ocean general circulation models to unravel forcing factors responsible for abrupt climate changes on millennial time scales during the Pleistocene, as demonstrated in Peltier et al. (2006).

ACKNOWLEDGMENTS

This work was supported by the Norwegian (Norges Forskningsrad), German (Deutsche Forschungsgemeinschaft), and Korean (Korea Research Council of Public Science and Technology, Ministry of Marine and Fisheries) Research Councils. This research used samples and data provided by the Integrated Ocean Drilling Program (IODP). We are grateful to R. Spielhagen, D. Darby, and one anonymous referee for formal reviews.

REFERENCES CITED

Astakhov, V., 2004, Middle Pleistocene glaciations of the Russian North: Quaternary Science Reviews, v. 23, p. 1285–1311, doi: 10.1016/j.quascirev.2003.12.011.

Bauch, D., Carstens, J., and Wefer, G., 1997, Oxygen isotope composition of living *Neogloboquadrina pachyderma* (sin.) in the Arctic Ocean: Earth and Planetary Science Letters, v. 146, p. 47–58, doi: 10.1016/S0012–821X(96)00211–7.

Bauch, H.A., Erlenkeuser, H., Helmke, J.P., and Struck, U., 2000, A paleoclimatic evaluation of marine isotope stage 11 in the high northern Atlantic (Nordic seas): Global and Planetary Change, v. 24, p. 27–39, doi: 10.1016/S0921–8181(99)00067–3.

Bischof, J., and Darby, D.A., 1997, Mid- to Late-Pleistocene ice drift in the western Arctic ocean: Evidence for a different circulation in the past: Science, v. 277, p. 74–78, doi: 10.1126/science.277.5322.74.

Brinkhuis, H., 21 others, and the Leg 302 Expedition Scientists, 2006, Episodic fresh surface waters in the Eocene Arctic Ocean: Nature, v. 441, p. 606–609, doi: 10.1038/nature04692.

Darby, D.A., Bischof, J.F., Spielhagen, R.F., Marshall, S.A., and Herman, S.W., 2002, Arctic ice export events and their potential impact on global climate during the late Pleistocene: Paleoceanography, v. 17, p. 15-1–15-17.

Dickson, R.R., Meincke, J., Malmberg, S.-A., and Lee, A.J., 1988, The "Great Salinity Anomaly" in the Northern North Atlantic 1968-1982: Progress in Oceanography, v. 20, p. 103–151, doi: 10.1016/0079-6611(88)90049-3.

Dyke, A.S., Andrews, J.T., Clark, P.U., England, J.H., Miller, G.H., Shaw, J., and Veillette, J.J., 2002, The Laurentide and Innuitian ice sheets during the Last Glacial Maximum: Quaternary Science Reviews, v. 21, p. 9–31, doi: 10.1016/S0277–3791(01)00095–6.

Flower, B.P., 1997, Overconsolidated section on the Yermak Plateau, Arctic Ocean: Ice sheet grounding prior to ca. 660 ka?: Geology, v. 25, p. 147–150, doi: 10.1130/0091–7613(1997)025<0147:OSOTYP>2.3.CO;2.

Flower, B.P., Oppo, D.W., McManus, J.F., Venz, K.A., Hodell, D.A., and Cullen, J.L., 2000, North Atlantic intermediate to deep water circulation and chemical stratification during the past 1 Myr: Paleoceanography, v. 15, p. 388–403, doi: 10.1029/1999PA000430.

Ganopolski, A., and Rahmstorf, S., 2001, Rapid changes of glacial climate simulated in a coupled climate model: Nature, v. 409, p. 153–158, doi: 10.1038/35051500.

Gascard, J.C., Watson, A.J., Messias, M.J., Olsson, K.A., Johannessen, T., and Simonsen, K., 2002, Long-lived vortices as a mode of deep ventilation in the Greenland Sea: Nature, v. 416, p. 525–527, doi: 10.1038/416525a.

Helmke, J.P., Bauch, H.A., and Erlenkeuser, H., 2003, Development of glacial and interglacial conditions in the Nordic seas between 1.5 and 0.35 Ma: Quaternary Science Reviews, v. 22, p. 1717–1728, doi: 10.1016/S0277–3791(03)00126–4.

Kristoffersen, Y., Coakley, B., Jokat, W., Edwards, M., Brekke, H., and Gjengedal, J., 2004, Seabed erosion on the Lomonosov Ridge, central Arctic Ocean: A tale of deep draft icebergs in the Eurasia Basin and the influence of Atlantic water inflow on iceberg motion?: Paleoceanography, v. 19, p. PA3006, doi: 10.1029/2003PA000985.

Lisiecki, L.E., and Raymo, M.E., 2005, A Pliocene-Pleistocene stack of 57 globally distributed benthic $\delta^{18}O$ records: Paleoceanography, v. 20, p. PA1003, doi: 10.1029/2004PA001071.

Lund, S., Stoner, J.S., Channell, J.E.T., and Acton, G., 2006, A summary of Brunhes paleomagnetic field variability recorded in Ocean Drilling Program cores: Physics of the Earth and Planetary Interiors, v. 156, p. 194–204, doi: 10.1016/j.pepi.2005.10.009.

Mudelsee, M., and Schulz, M., 1997, The Middle Pleistocene climate transition: Onset of 100 kyr cycle lags ice volume buildup by 280 ka: Earth and Planetary Science Letters, v. 151, p. 117–123, doi: 10.1016/S0012–821X(97)00114–3.

Myhre, A., Thiede, J., and Firth, J.A., 1995, Proceedings of the Ocean Drilling Program, Initital reports, Leg 151, College Station, Texas, Ocean Drilling Program, 951 p.

Nørgaard-Pedersen, N., Spielhagen, R.F., Erlenkeuser, H., Grootes, P.M., Heinemeier, J., and Knies, J., 2003, Arctic Ocean during the Last Glacial Maximum: Atlantic and polar domains of surface water mass distribution and ice cover: Paleoceanography, v. 18, p. 1063, doi: 10.1029/2002PA000781.

Peltier, W.R., Vettoretti, G., and Stastna, M., 2006, Atlantic meridional overturning and climate response to Arctic Ocean freshening: Geophysical Research Letters, v. 33, L06713, doi: 10.1029/2005GL025251.

Peterson, B.J., McClelland, J., Curry, R., Holmes, R.M., Walsh, J.E., and Aagaard, K., 2006, Trajectory shifts in the Arctic and subarctic freshwater cycle: Science, v. 313, p. 1061–1066, doi: 10.1126/science.1122593.

Raymo, M.E., Oppo, D.W., Flower, B.P., Hodell, D.A., McManus, J.F., Venz, K.A., Kleiven, K.F., and McIntyre, K., 2004, Stability of North Atlantic water masses in face of pronounced climate variability during the Pleistocene: Paleoceanography, v. 19, p. PA2008, doi: 10.1029/2003PA000921.

Rise, L., Olesen, O., Rokoengen, K., Ottesen, D., and Riis, F., 2004, Mid-Pleistocene ice drainage pattern in the Norwegian Channel imaged by 3D seismic: Quaternary Science Reviews, v. 23, p. 2323–2335, doi: 10.1016/j.quascirev.2004.04.005.

Spielhagen, R.F., Baumann, K.-H., Erlenkeuser, H., Nowaczyk, N.R., Norgaard-Pedersen, N., Vogt, C., and Weiel, D., 2004, Arctic Ocean deep-sea record of northern Eurasian ice sheet history: Quaternary Science Reviews, v. 23, p. 1455–1483, doi: 10.1016/j.quascirev.2003.12.015.

Svendsen, J.I., Alexanderson, H., Astakhov, V.I., Demidov, I., Dowdeswell, J.A., Funder, S., Gataullin, V., Henriksen, M., Hjort, C., Houmark-Nielsen, M., Hubberten, H.W., Ingolfsson, O., Jakobsson, M., Kjnær, K.H., Larsen, E., Lokrantz, H., Lunkka, J.P., Lysa, A., Mangerud, J., Matiouchkov, A., Murray, A., Moller, P., Niessen, F., Nikolskaya, O., Polyak, L., Saarnisto, M., Siegert, C., Siegert, M.J., Spielhagen, R.F., and Stein, R., 2004, Late Quaternary ice sheet history of northern Eurasia: Quaternary Science Reviews, v. 23, p. 1229–1271, doi: 10.1016/j.quascirev.2003.12.008.

Tarasov, L., and Peltier, W.R., 2005, Arctic freshwater forcing of the Younger Dryas cold reversal: Nature, v. 435, p. 662–665, doi: 10.1038/nature03617.

Manuscript received 23 April 2007
Revised manuscript received 10 July 2007
Manuscript accepted 16 July 2007

Printed in USA